Eur. Phys. J. D **6**, 269–279 (1999)

THE EUROPEAN PHYSICAL JOURNAL D

EDP Sciences

Experimental study for the optimization of plasma torch operations

R. Benocci[1], R. Florio[1], A. Galassi[1], M. Paolicchio[1], M. Piselli[1], C. Sala[1], M. Sciascia[1], and E. Sindoni[2,a]

[1] Dipartimento di Fisica, sez. Plasmi, Via Celoria 16, 20133 Milano, Italy
[2] Dipartimento di Scienze dell'Ambiente e del Territorio, Via Emanueli 15, Milano, Italy

Received: 20 November 1998 / Received in final form: 11 December 1998

Abstract. In this paper the electric and efficiency attributes of a low-powered dc plasma torch has been investigated. Torch operations require reproducibility, reliability and economicity to be attained. The characterisation allowed to scope operative ranges on the basis of minimum voltage fluctuations and maximum thermal efficiency levels for different gas flow rates, anode dimensions, arc current and two process gases (Ar, N_2).

PACS. 52.75.Hn Plasma torches. – 52.75.Rx Plasma applications in manufacturing and materials processing (etching, surface cleaning, spraying, arc welding, ion implantation, film deposition, etc.).

1 Introduction

It is well recognised that the full potential of plasma technology depends on the ability to achieve the optimal match between the process requirements, the characteristics of the plasma source and the reactor design used. To this purpose, a 30 kW power supplied arc plasma torch has been entirely designed and carried out. The torch optimization requires the investigation of the parameters determining its structural design and operative condition. The major interest concerns the following parameters:

- process gas composition,
- gas flow rate,
- electric power supply,
- arc current,
- anode dimensions.

These parameters are not completely disrelated: some of them are linked by constructional design, structural parameters (electrode dimensions and configuration, gas-injection geometry, maximum gas flow rate,...); others depend on the operative mode of the torch (power, type of gas, flow rate,...) and are connected by relations so that once a parameter has been chosen, restrictions occur for the others [1,2].

The optimum operative parameters, in this work, have been determined investigating the electrical characteristics and thermal efficiency of the torch system.

[a] e-mail: sindoni@alpha.disat.unimi.it

2 Experimental set-up

The experimental apparatus employed for the torch characterization is depicted in Figure 1. The plasma torch used in the experiment is a non-transferred dc arc torch [3].

It has a typical spray configuration: a tungsten rod-shaped, water-cooled cathode ($D_c = 5\,\mathrm{mm}$ diameter, 60° conical tip) and a water-cooled, coaxial, cylindrical, copper anode (nozzle channel length 30 mm, cone angle 60°). The cathode-anode distance is 1.5 mm. The process gas (argon or nitrogen) is axially injected into the discharge reactor upstream the cathode through an annular aperture surrounding the cathode holder. Its dimension allows feeding up to 300 slm (N_2, Ar). This arrangement should avoid motion of the cathode arc attachment, thus stabilizing arc operations.

The gas flow rate is controlled via a fine manual valve; a flow meter coupled with a mixer, settled downstream the valve, regulates the injected process gas.

Each electrode is provided with an independent water cooling circuit. The flow rate is mastered via two flow meters and the temperature rise between the inlet and outlet cooling water of the reactor is measured by thermocouples of type T. The power released on each electrode is calculated by the following energy balance equation:

$$Q_{\mathrm{el}} = \dot{m}_{\mathrm{w}} C_p (T_{\mathrm{out}} - T_{\mathrm{in}})\,, \qquad (1)$$

where $\dot{m}_{\mathrm{w}}$ is the water mass flow rate, C_p the water specific heat at constant pressure, T_{out} and T_{in} the outlet and inlet temperatures, respectively. The heat losses in the cooling circuit between the reactor and the thermocouples mounting have been minimized adopting insulated pipelines.

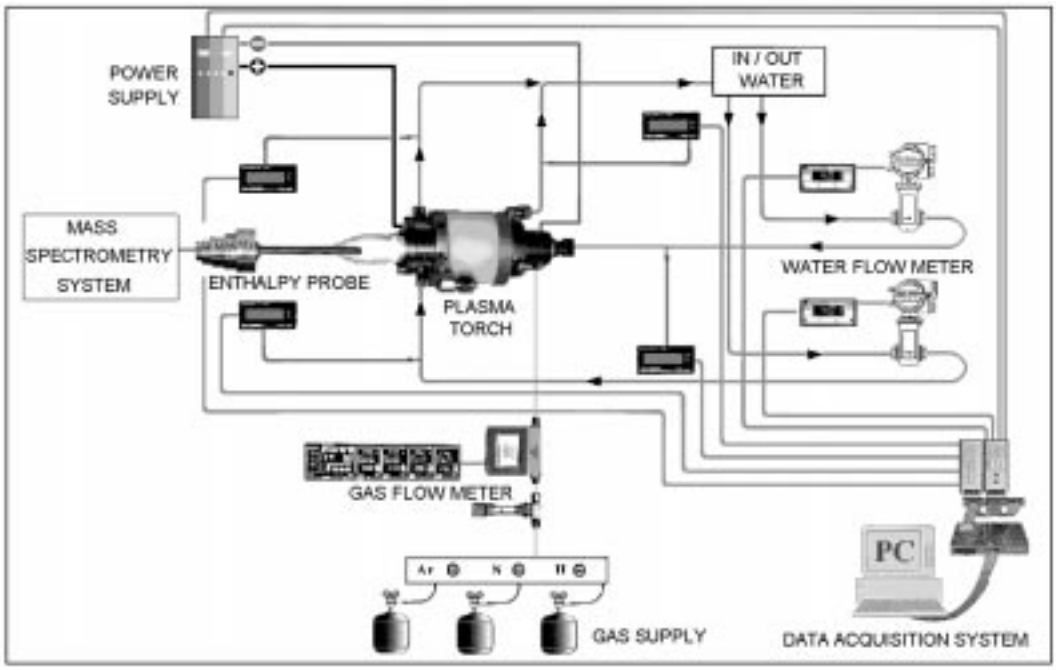

Fig. 1. Experimental set-up.

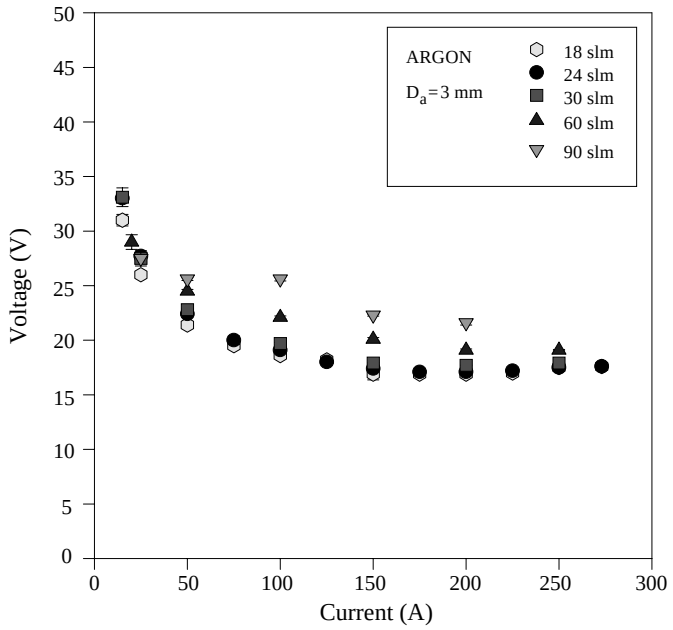

Fig. 2. Voltage drop *versus* arc current for different argon flow rates and anode internal diameter 3 mm.

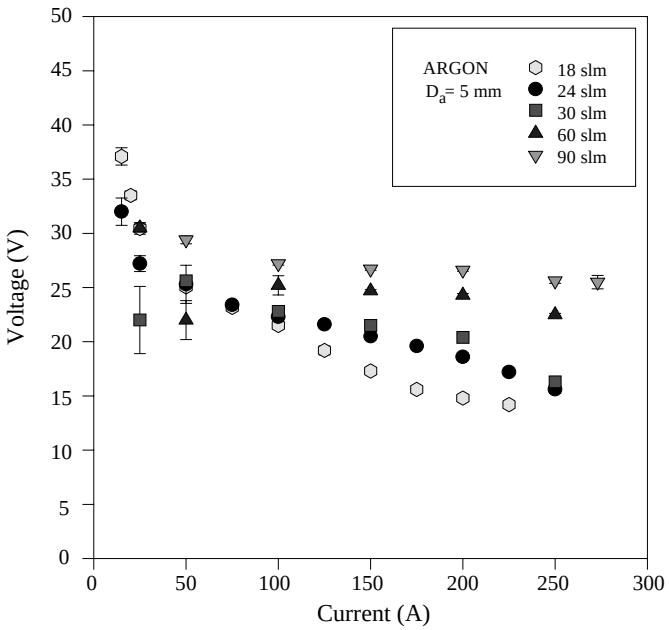

Fig. 3. Voltage drop *versus* arc current for different argon flow rates and anode internal diameter 5 mm.

Arc stabilization and fluctuation in different operative conditions has been studied by monitoring potential variations.

The torch thermal efficiency η is determined as the ratio between the power dissipated into the plasma column (Q_{plasma}) and the power supplied to the torch ($V_{\text{arc}} \cdot I$):

$$\eta = \frac{Q_{\text{plasma}}}{V_{\text{arc}} \cdot I} = 1 - \frac{Q_{\text{el}}}{V_{\text{arc}} \cdot I} \tag{2}$$

being $Q_{\text{el}} = Q_{\text{el}}^{\text{cathode}} + Q_{\text{el}}^{\text{anode}}$ measured by equation (1).

3 Experimental procedure

Anode diameters of 3, 4, 5 and 6 mm have been used.

Attention has been addressed to the following torch characteristics:

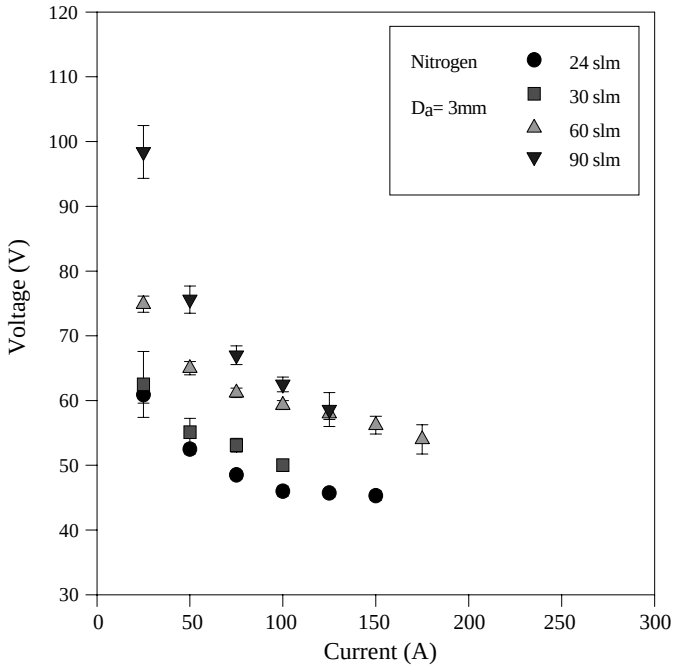

Fig. 4. Voltage drop as a function of current for different nitrogen flow rates and anode internal diameter 3 mm.

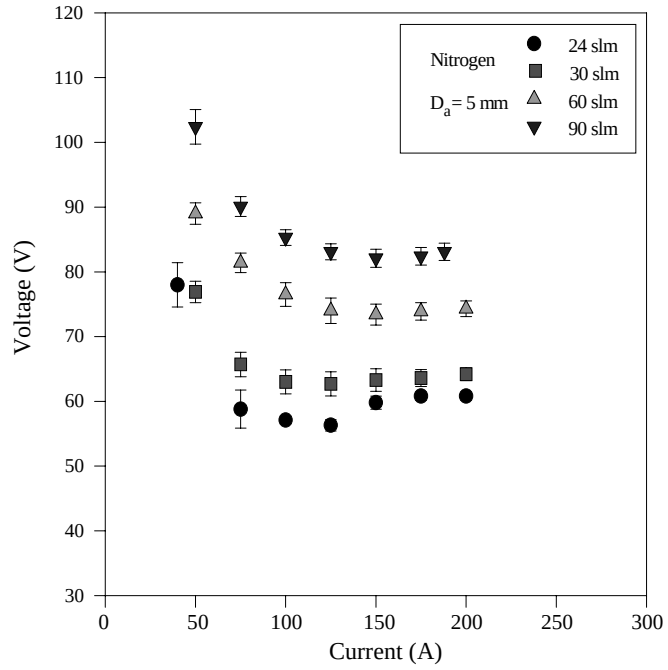

Fig. 5. Voltage drop *versus* arc current for different argon and nitrogen flow rates, anode internal diameter 5 mm.

1. Current-voltage characteristics for different operative and structural parameters.
2. Thermal efficiency evolution *versus* operative and structural parameters.
3. Restrike and arc stability (peak-to-peak values of the typical saw-tooth voltage fluctuations and error bars evolution).

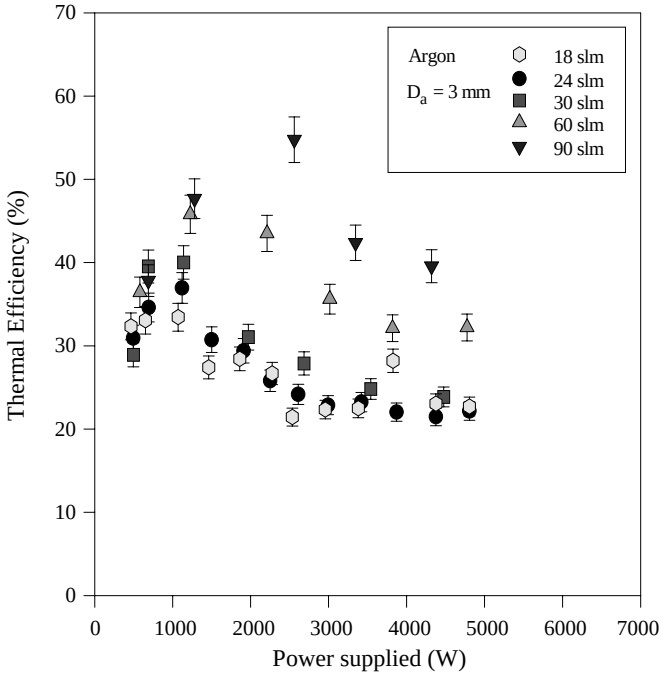

Fig. 6. Thermal efficiency *versus* power supplied for different argon flow rates, anode internal diameter 3 mm (5% error is displayed).

The experiment has been performed with the following procedure:

- choice of anode diameter (from 6 to 3 mm),
- choice of gas nature (argon or nitrogen),
- for a fixed gas flow rate (from low to high flow rates), current scan on the entire available range (10–275 A).

Water flow rates in the electrodes cooling circuit have been set 1.2 l/m and 2.5 l/m for cathode and anode, respectively.

4 Current-voltage characteristics

The electrical characterization of the torch requires the knowledge of the voltage drop as a function of arc current. In Figures 2 and 3 current-voltage characteristics are reported for anode diameters of 3 and 5 mm and different argon gas flow rates.

The potential difference at the electrode ends presents a decreasing evolution as the arc current rises. In particular, at low currents, the voltage exhibits a steep change that reveals to be higher at lower gas flow rates. In Figure 2, for currents greater than 150 A, the potential difference tends to flatten. Diameter of 5 mm (Fig. 3) presents a decreasing tendency for all the monitored gas flow rates (only a flattening trend for 60 and 90 slm and currents $I > 150$ A) and on the entire range of current. This behaviour can be attributed to different interaction conditions between the gas and the electric arc. In general, at low currents and high gas flow rates, the electric arc partially interacts with the process gas due to its reduced

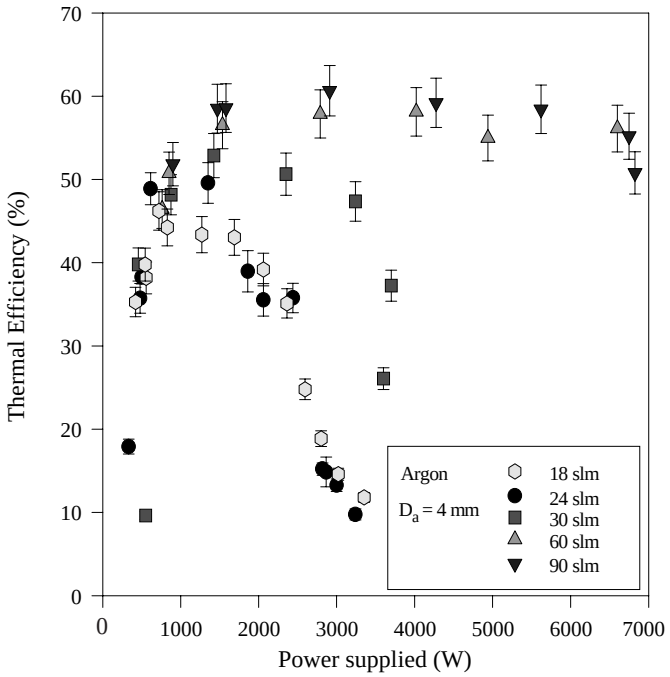

Fig. 7. Thermal efficiency *versus* power supplied for different argon flow rates, anode internal diameter 4 mm (5% error is displayed).

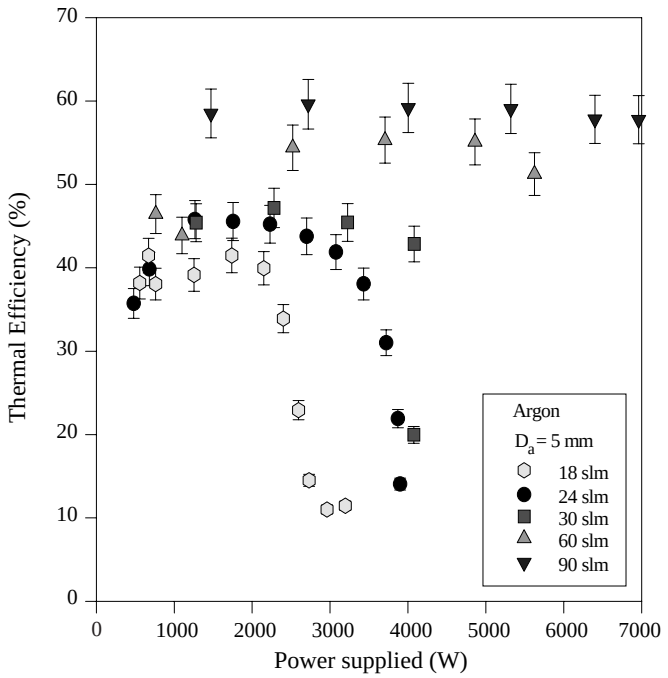

Fig. 8. Thermal efficiency *versus* power supplied for different argon flow rates, anode internal diameter 5 mm (5% error is displayed).

dimensions, giving rise to turbulence and consequently instabilities. At higher currents the arc dimension grows producing a better coupling with the process gas even at high gas flow rates. This phenomenon causes a change of the temperature distribution in the arc column that requires the voltage to adjust to sustain a fixed arc current. Increasing the anode dimension causes an offset of the described process at higher currents and lower gas flow rates.

It is worth noting that, for a fixed arc current, an increase of the gas flow rate brings about a higher voltage drop. Such a phenomenon can be ascribed to the arc stretching due to the presence of the gas flow acting on the arc attachment that originates a drag force.

As in the case of argon, two kinds of voltage evolution can be distinguished for nitrogen: the first one presents a decreasing current-voltage characteristic; the second one shows a rising of the voltage drop, as the gas flow rate increases (Figs. 4 and 5). This latter tendency confirms that, for a fixed arc current, higher amounts of gas cause greater drag forces and thus a higher arc stretching with corresponding higher voltages.

These data show a higher arc sensitivity to gas flow changes at low currents with respect to those at higher currents (for $I > 75$ A) and with small anode diameters, featuring an explicit and almost regular trend.

Nitrogen reveals a voltage drop doubled with respect to argon in the same operative conditions. Such a discrepancy can surely be attributed to thermodynamic and transport properties that originate different temperature distributions inside the plasma column. In particular the molecular nature of nitrogen is the basic issue explaining the different behaviour: the enthalpy peak in correspondence of nitrogen dissociation temperature ($\cong$ 6500 K) requires, for a fixed arc current, a higher power supplied to sustain a nitrogen than an argon arc [4].

5 Thermal efficiency

Thermal efficiency measurements have been performed with the following experimental procedure: once the process gas and flow rate have been fixed, the arc current is set and the heat dissipated in the cooling system is calculated by evaluating the temperature rise in stationary conditions. The thermal efficiency is thus reckoned using equation (2). In addition the choice of displaying the experimental thermal efficiencies as a function of the power supplied is justified by the fact that the voltage drop is not a free parameter being linked, besides to the operative parameters, to the structural parameters of the torch. Hence the power supplied represents a more significant parameter than the current alone.

Figure 6 shows the evolution of thermal efficiency as a function of power supplied in case of argon and $D_a = 3$ mm; the efficiencies are quite low and present maxima. At 18 slm the maximum is less than 35% at a supplied power of 1 kW. The efficiency peak rises as the flow rate is increased reaching 45% at 1.3 kW and 60 slm, and 55% at 2.5 kW and 90 slm. Thermal efficiencies as a function of power supplied evolve to a saturation profile increasing anode diameters, for gas flow rates greater than 30 slm as shown in Figures 7-9. This typical shape with maxima is not evidenced for nitrogen (Figs. 10-13). As the power

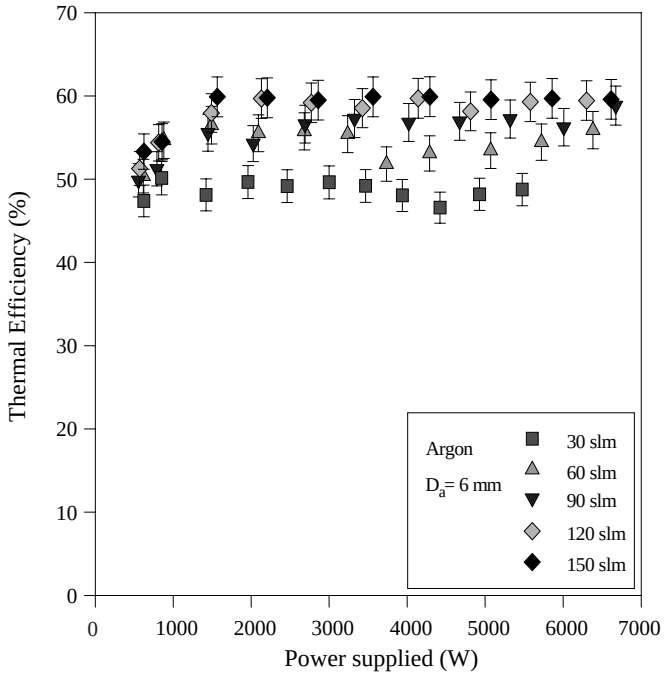

Fig. 9. Thermal efficiency *versus* power supplied for different argon flow rates, anode internal diameter 6 mm (5% error is displayed).

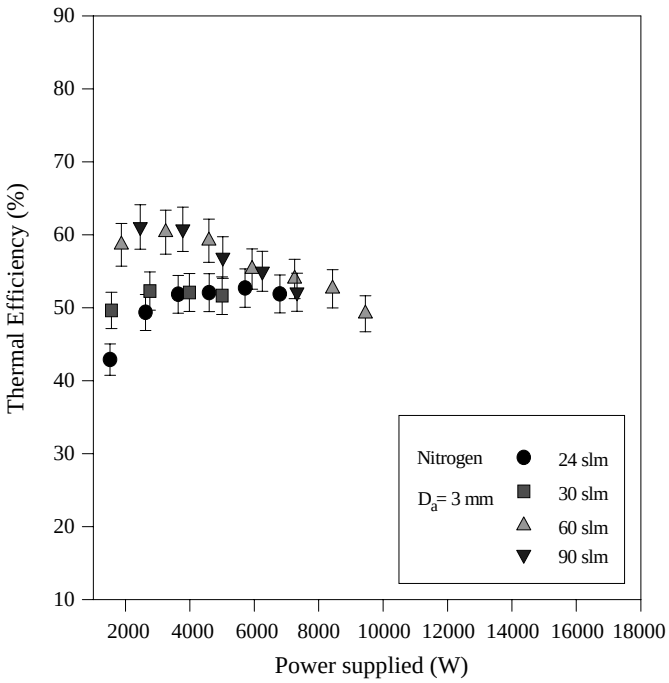

Fig. 10. Thermal efficiency *versus* power supplied for different nitrogen flow rates, anode internal diameter 3 mm (5% error is displayed).

gets up, for a fixed gas flow rate, the combination of the current-voltage characteristic and the power loss through the electrodes is at the origin of this phenomenon, being the power loss an increasing function of the power supplied (Figs. 14 and 15 for argon and nitrogen, $D_{\rm a} = 3,5$ mm). In particular the efficiency trend is driven by the rate of variation of the heat loss and the power supplied as a function of current. The thermal efficiency for nitrogen exceeds by about 35–50% that for argon. The anode heat load largely exceeds that for the cathode as shown in Figures 16 and 17 for argon and nitrogen and anode diameter of 5 mm.

6 Voltage fluctuation and arc stability

A blown arc striking in a tubular anode undergoes aerodynamic forces that cause arc stretching. When the arc column is sufficiently elongated and, consequently, its potential difference is increased, a breakdown between the arc and the anode occurs and another arc attachment is created [5].

This phenomenon, known as restrike mode of the arc, can cause voltage fluctuations as high as 90% of the mean voltage drop between the two electrodes. Typical voltage waveforms are shown in Figures 18 and 19 for argon and nitrogen. The analysis of arc fluctuations and instabilities has been accomplished recording peak-to-peak (P-P) voltage and the associated standard deviation (~ 100 events for each value). In the case of argon, experimental data reveal a reduction of P-P potentials as the arc current is raised and an increase with higher gas flow rate (see Figs. 20 and 21). Low currents ($I < 50$ A) make the arc more sensitive to gas flow rate changes; this means that when the current rises the arc gets thicker resulting in a higher inertia. The arc dimension can be affected by the operative parameters of a torch: arc current and gas flow rate. In fact an arc current increase originates a temperature distribution change, resulting in enhanced arc dimension. The gas flow rate acts modifying the heat exchanged by convection between arc and gas, thus influencing the arc dimension as well.

The arc elongation depends on the anode diameter. This can be attributed to a minor distance between the arc and anode wall, thus requiring a lower potential difference to cause a breakdown (see Fig. 22).

Here again, the non-linear behaviour of all the transport and thermodynamic properties for nitrogen in the temperature range 5000-8000 K and, in particular, of the thermal conductivity and the specific heat at constant pressure, give rise to voltage fluctuations as high as one order of magnitude greater than the argon (see Figs. 23 and 24 for $D_{\rm a} = 3$ and 5 mm, respectively) and are responsible for different arc cross-sections testifying also two different modes for the generation of fluctuations observed as wave-like and jumps (see Figs. 18 and 19).

The first, typical of monatomic gases, is originated by the diffused and not shaped arc attachment and due to the almost linear dependence of thermal conductivity on the temperature. The second, typical of molecular gases, is due to the presence of peaks in the thermal conductivity corresponding to temperatures where molecules begin to dissociate [4,6].

In addition the corresponding error bars associated to P-P data reveal a reduction with the current and anode

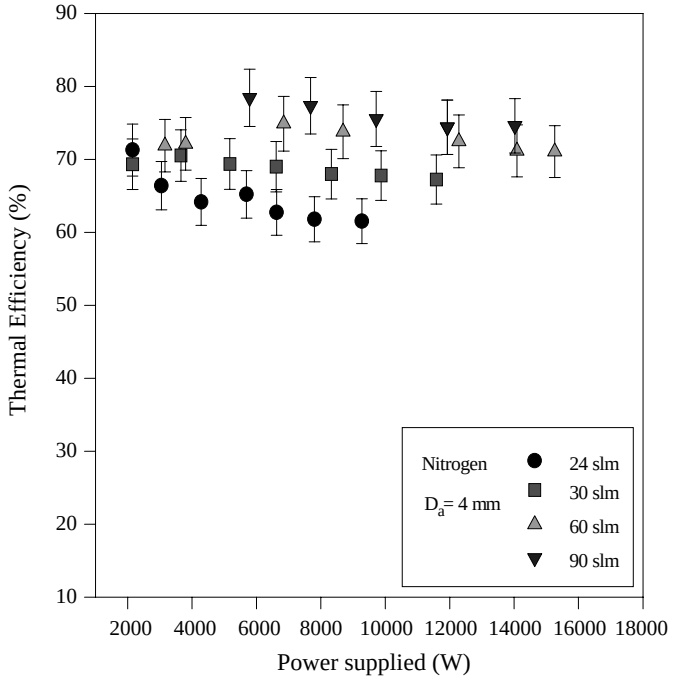

Fig. 11. Thermal efficiency *versus* power supplied for different nitrogen flow rates, anode internal diameter 4 mm (5% error is displayed).

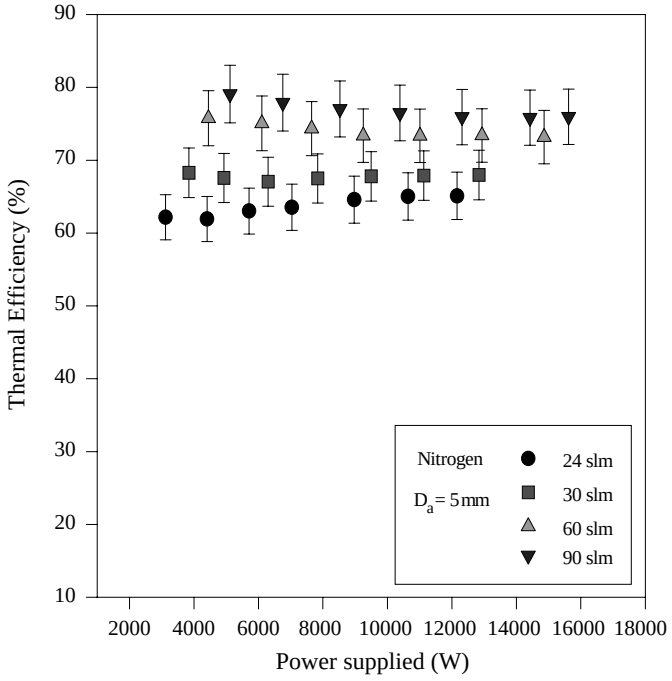

Fig. 12. Thermal efficiency *versus* power supplied for different nitrogen flow rates, anode internal diameter 5 mm (5% error is displayed).

diameter for both argon (Figs. 25 and 26) and nitrogen (Figs. 27 and 28). These results show that the effect of a higher arc current and smaller anode diameters is to make the arc less sensitive to given flow conditions and provide condition of better arc stability.

7 Discussion of results

The analysis of the torch performances is based on the electrical and energy balance (thermal efficiency) behaviour under different operational and structural modes.

In order to make a plasma technology profitable, high thermal efficiencies are requested, although this is not the only parameter affecting torch operations. The presence of voltage fluctuations can cause temperature distribution variations that, in some cases, may disturb or even hamper the success of a process [6].

An interpretation scheme of experimental electrical and calorimetric data is proposed, in order to scope convenient operative ranges, matching process requirements and plasma source characteristics.

The following pattern is employed to limit the range of operative parameters for fixed gas nature, gas flow rate and anode diameter:

1. Position of maximum values of thermal efficiency η_{MAX}.
2. Values of η not less than 10% of η_{MAX} and determination of the correspondent current intensity range ΔI_{η}.
3. Choice of current intensity range $\Delta I_{\mathrm{P\text{-}P}}$ for which P-P voltage gets "constant" ($I \in \Delta I_{\mathrm{P\text{-}P}} \Leftrightarrow \frac{|\overline{V}_{\mathrm{P\text{-}P}} - V_{\mathrm{P\text{-}P}}|}{\overline{V}_{\mathrm{P\text{-}P}}} \times 100 \lesssim$ 20–30%, where $\overline{V}_{\mathrm{P\text{-}P}}$ is calculated over the current range $\Delta I_{\mathrm{P\text{-}P}}$).
4. Choice of current intensity range ΔI_{sd} for which error bars voltage get "constant" ($I \in \Delta I_{\mathrm{sd}} \Leftrightarrow \frac{|\overline{V}_{\mathrm{sd}} - V_{\mathrm{sd}}|}{\overline{V}_{\mathrm{sd}}} \times 100 \lesssim$ 20–30%, where $\overline{V}_{\mathrm{sd}}$ is calculated over the current range ΔI_{sd}).
5. Intersection between ranges of current defining the Current at Best Operative Conditions (CBOC).
6. Determination of the corresponding Power Supplied at Best Operative Conditions (PSBOC).
7. η_{MAX} corresponding to CBOC.
8. Maximum voltage fluctuation corresponding to CBOC.
9. Maximum P-P uncertainty value corresponding to CBOC.

Condition 4. establishes working conditions excluding intermittency operations and leading to voltage fluctuations considered as stationary. Both in case of argon and nitrogen, a gas flow rate of 60 slm seems to guarantee acceptable relative values of efficiency for all diameters. Operative current ranges go up with diameters as well as voltage fluctuations. An increase of thermal efficiency is also observed as the anode diameter is enlarged. This is in connection with the higher voltage fluctuations that make the heat losses throughout the anode inferior due to a better distribution of the heat dissipated on the system anode-process gas. In addition the presence of a larger sheath gas layer also assures a good thermal insulation between the arc and the anode surface, even though it tends to reduce process gas-arc interaction.

$D_{\mathrm{a}} = 3\,\mathrm{mm}$: The analysis of results shows that, in case of argon, η_{MAX} is rather small ($\eta_{\mathrm{MAX}} = 45.8\%$,

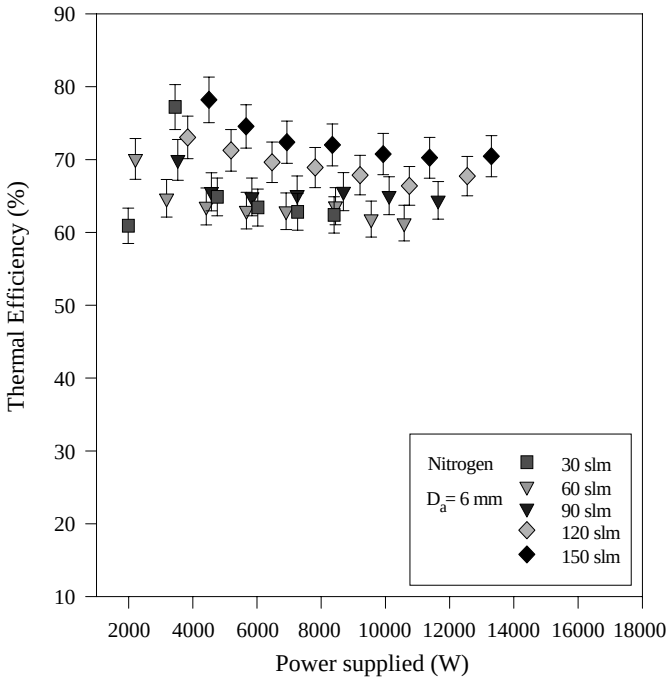

Fig. 13. Thermal efficiency *versus* power supplied for different nitrogen flow rates, anode internal diameter 6 mm (5% error is displayed).

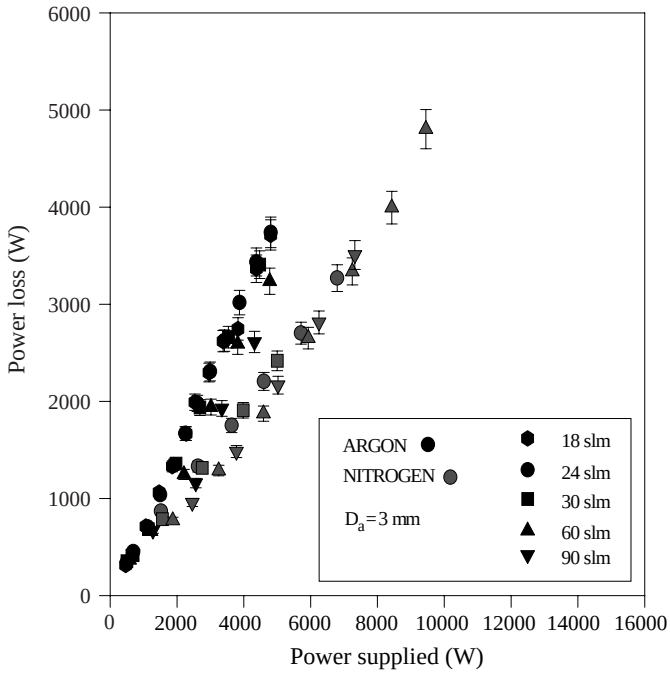

Fig. 14. Power loss *versus* power supplied for different argon and nitrogen flow rates and $D_a = 3\,\text{mm}$.

CBOC 25–100 A at 60 slm) with relative low voltage fluctuations and regularity of displacement (7.1 and 3%, respectively, at 60 slm). Nitrogen gives higher efficiency ($\eta_{MAX} = 60.3\%$, CBOC 25–100 A at 60 slm) but strong fluctuations (70.2%).

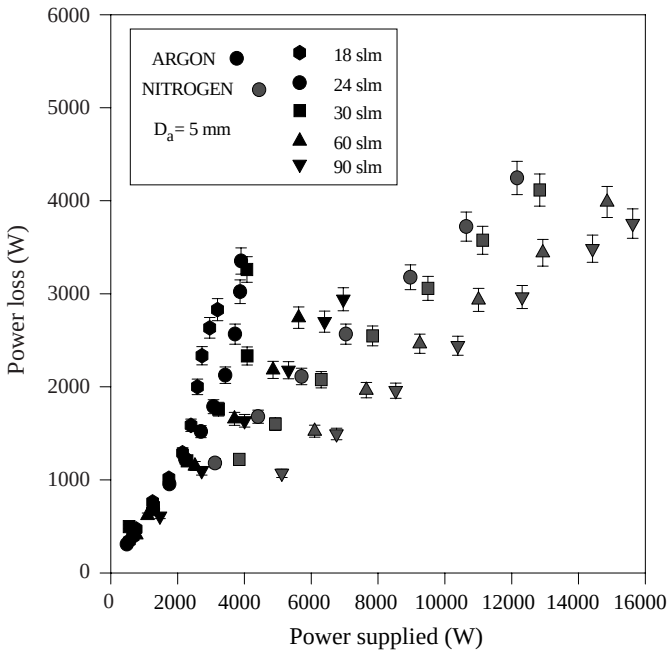

Fig. 15. Power loss *versus* power supplied for different argon and nitrogen flow rates and $D_a = 5\,\text{mm}$.

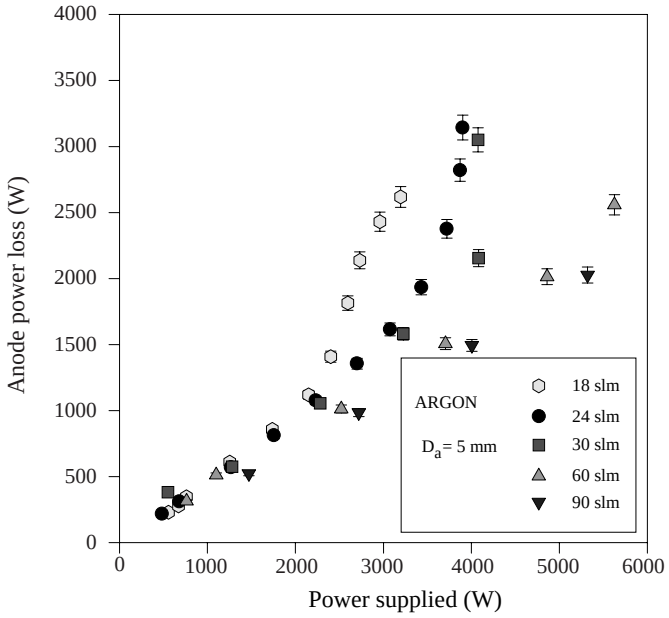

Fig. 16. Anode power loss *versus* power supplied for different argon flow rates and $D_a = 5\,\text{mm}$.

$D_a = 4\,\text{mm}$: Acceptable compromise is obtained at 30 slm for argon ($\eta_{MAX} = 52.8\%$, CBOC 50–150 A); fluctuations can be considered as stationary. Nitrogen best operative condition is matched at 30–60 slm with $\eta_{MAX} = 70.5$–72.4%, but with fluctuations as high as 90% of the average voltage drop.

$D_a = 5\,\text{mm}$: In case of argon, a gas flow rate of 60 slm is suggested ($\eta_{MAX} = 55.3\%$, CBOC 100–250 A); for nitrogen at 90 slm ($\eta_{MAX} = 78\%$, CBOC >50–188 A, voltage fluctuation 76.1%).

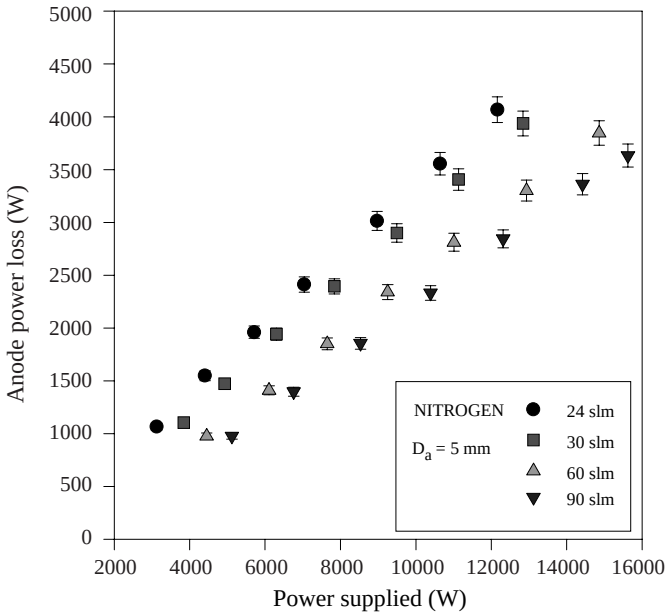

Fig. 17. Anode power loss *versus* power supplied for different nitrogen flow rates and $D_a = 5\,\text{mm}$.

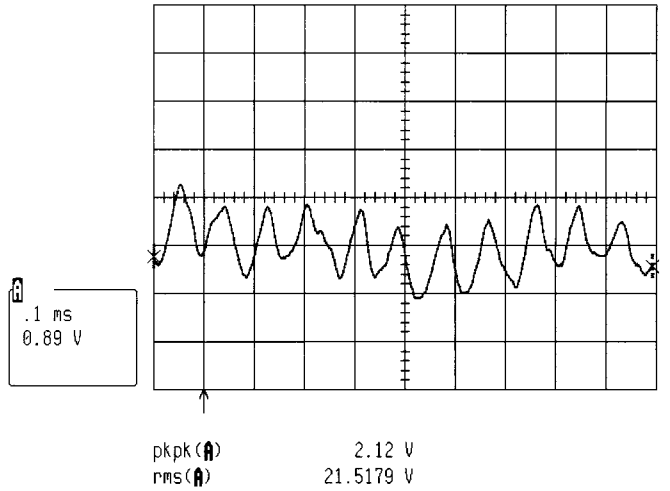

Fig. 18. Voltage waveform for argon.

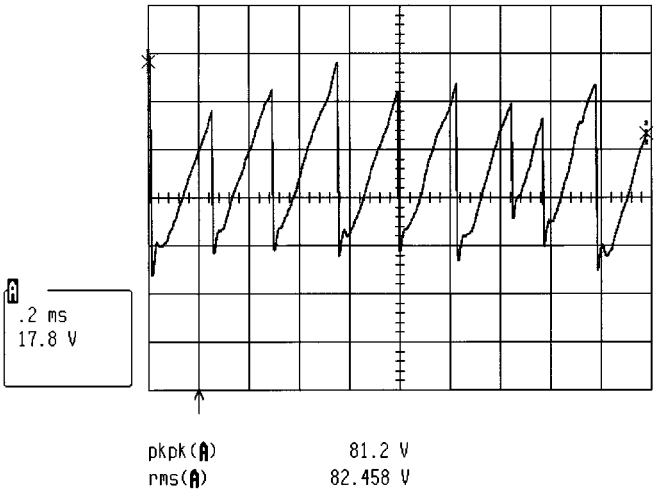

Fig. 19. Voltage waveform for nitrogen.

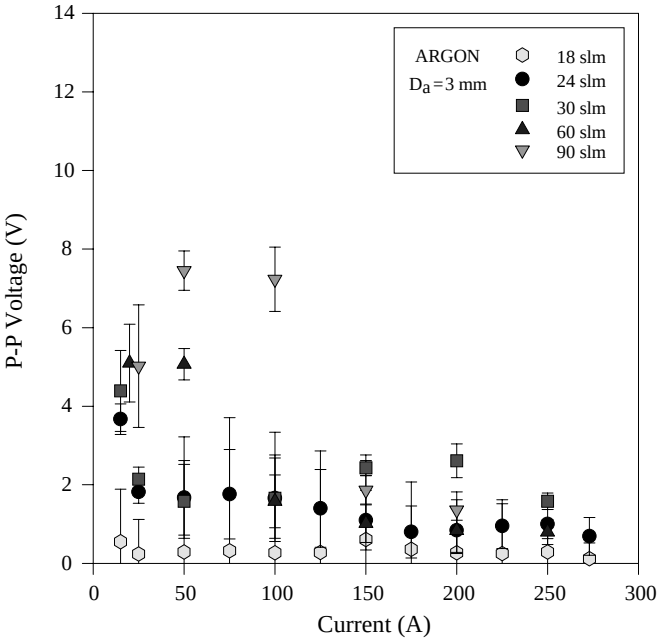

Fig. 20. Peak-to-peak voltage *versus* arc current for different argon flow rates and $D_a = 3\,\text{mm}$.

$D_a = 6\,\text{mm}$: The use of argon presents an increase of voltage fluctuation as much as twice the one observed in the other cases, but with a substantially unchanged thermal efficiency. Nitrogen reveals worse performances, for the same working condition with $D_a = 5\,\text{mm}$; the same level of efficiency is reached at 150 slm but with a doubled voltage fluctuation.

8 Conclusions

In this work the analysis of the characteristics of a low-powered plasma torch has been approached investigating the electric and efficiency attributes of the reactor. The results allowed to scope operative ranges on the basis of minimum stationary voltage fluctuations and maximum thermal efficiency levels for different gas flow rates and two process gases (Ar, N_2). This is an important issue that can not be ignored when technological processes require reproducibility, reliability and economicity.

Appendix

The error in the efficiency determination depends on the instrumentation precision used for water flow rate m_w, current I, mean arc voltage V_{arc} and cooling water temperature rise measurements ($T_{out} - T_{in}$). The thermal efficiency requires the following measurements: anode and cathode water flow rate and temperature rise, current intensity and voltage drop. Indicating with $\delta X/X$ the

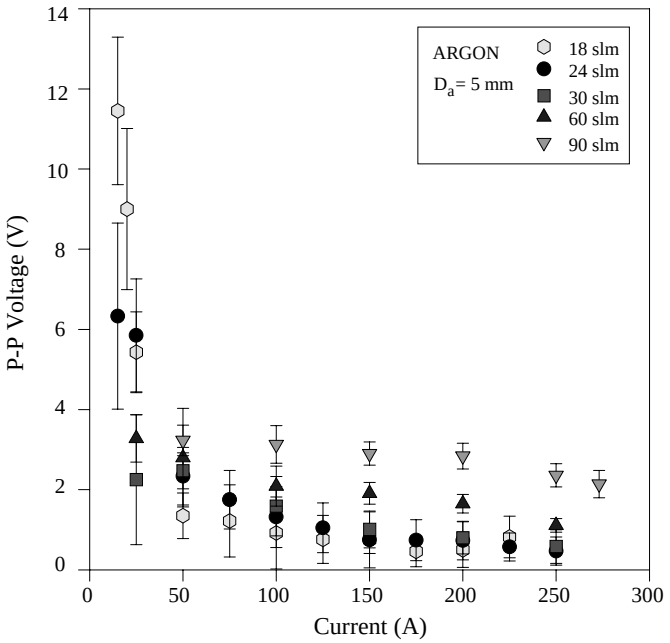

Fig. 21. Peak-to-peak voltage *versus* arc current for different argon flow rates and $D_{\rm a} = 5\,{\rm mm}$.

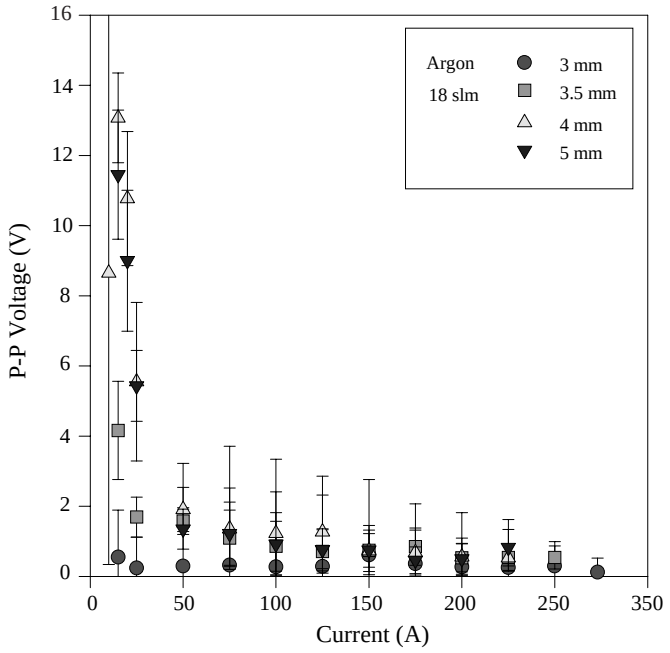

Fig. 22. Peak-to-peak voltage *versus* arc current for different anode internal diameter and argon flow rate 18 slm.

relative error associated to the quantity X, the error on the efficiency is given by standard error analysis:

$$\left(\frac{\delta\eta}{\eta}\right)^2 = \left(\frac{\delta V}{V}\right)^2 + \left(\frac{\delta I}{I}\right)^2 + \left(\frac{\delta Q_{\rm anode}}{Q_{\rm anode}}\right)^2 + \left(\frac{\delta Q_{\rm cathode}}{Q_{\rm cathode}}\right)^2, \quad \text{(A.1)}$$

Although voltage and current errors are independent of

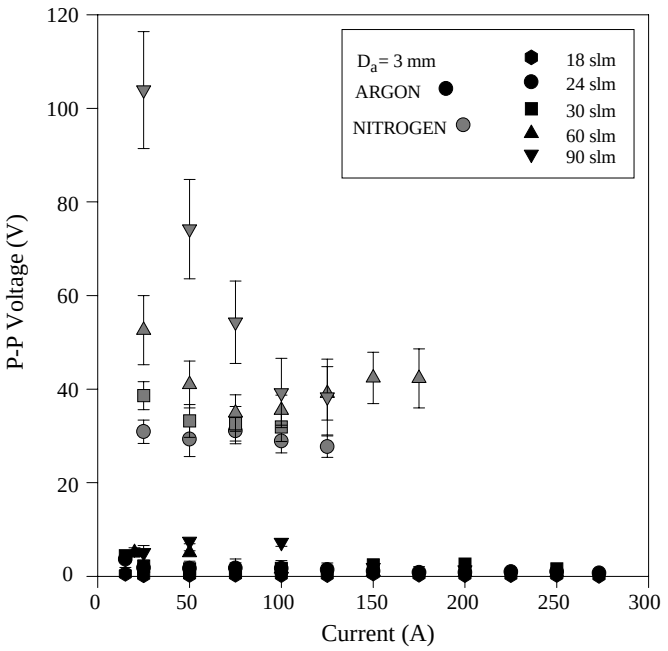

Fig. 23. Peak-to-peak voltage *versus* arc current for different nitrogen and argon flow rates and anode internal diameter $D_{\rm a} = 3\,{\rm mm}$.

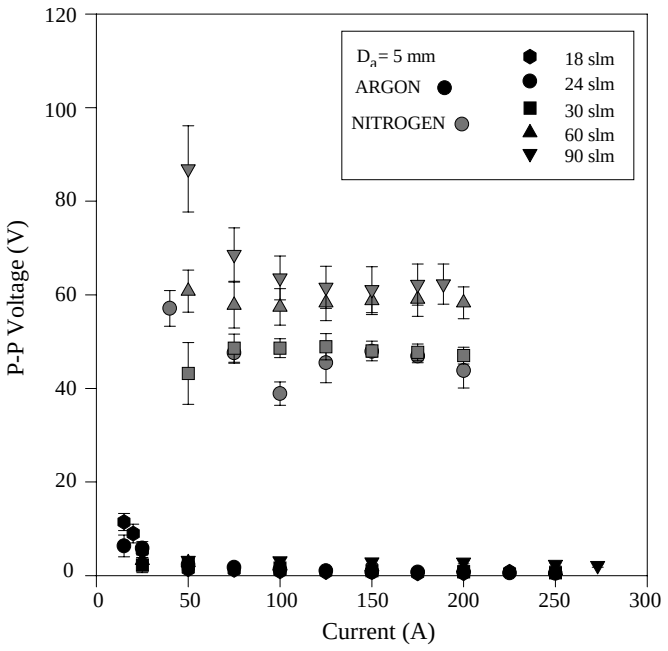

Fig. 24. Peak-to-peak voltage *versus* arc current for different nitrogen and argon flow rates and anode internal diameter $D_{\rm a} = 5\,{\rm mm}$.

operative conditions (*i.e.* 1%, on average, and 2%, respectively), errors relative to calorimetric measurement strongly depend on the amount of heat released on the electrodes; the efficiency error is therefore function of the power supplied to the torch. This behaviour is explained

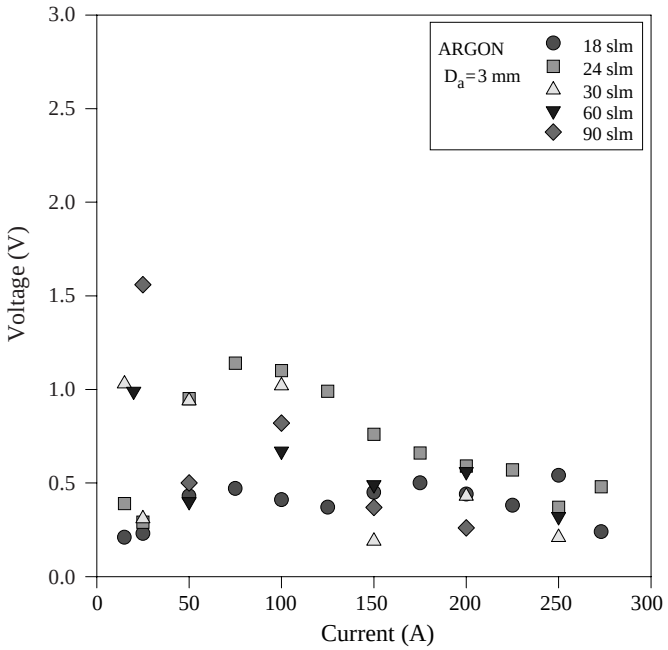

Fig. 25. P-P voltage error bars as a function of the arc current for different argon flow rates and anode internal diameter $D_\mathrm{a} = 3\,\mathrm{mm}$.

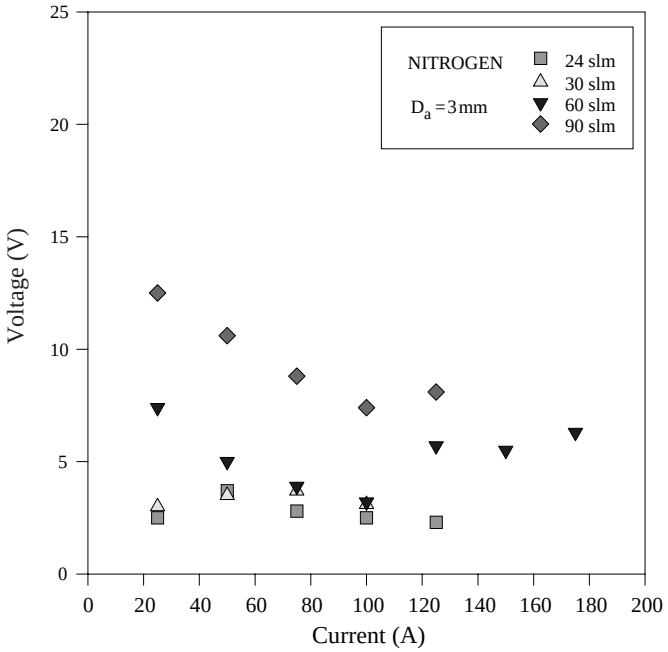

Fig. 27. P-P voltage error bars as a function of the arc current for different nitrogen flow rates and anode internal diameter $D_\mathrm{a} = 3\,\mathrm{mm}$.

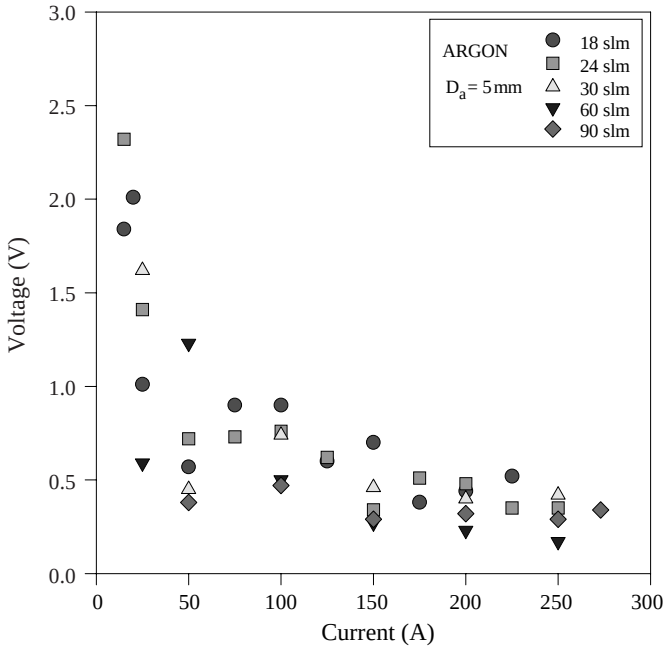

Fig. 26. P-P voltage error bars as a function of the arc current for different argon flow rates and anode internal diameter $D_\mathrm{a} = 5\,\mathrm{mm}$.

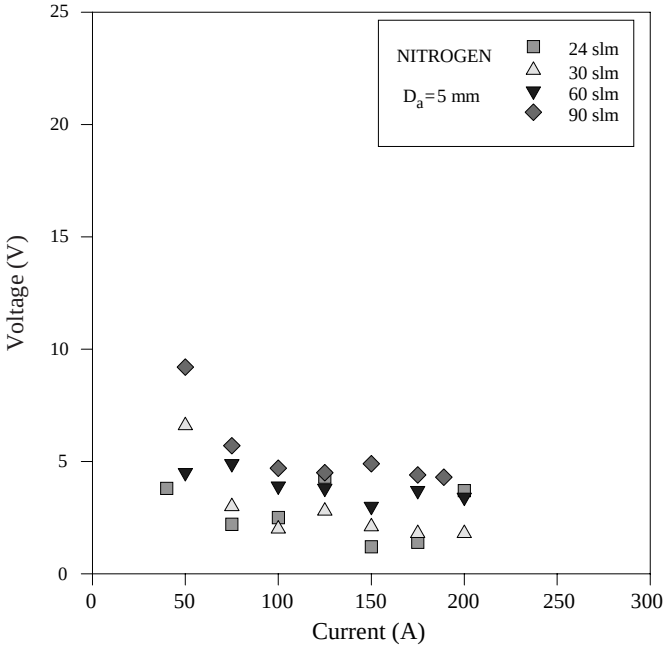

Fig. 28. P-P voltage error bars as a function of the arc current for different nitrogen flow rates and anode internal diameter $D_\mathrm{a} = 5\,\mathrm{mm}$.

by writing:

$$\left(\frac{\delta Q}{Q}\right)^2 = \left(\frac{\delta \Delta T}{\Delta T}\right)^2 + \left(\frac{\delta \dot{m}_\mathrm{w}}{\dot{m}_\mathrm{w}}\right)^2 . \qquad \text{(A.2)}$$

$\delta\dot{m}_\mathrm{w}/\dot{m}_\mathrm{w}$ is constant (0.5%) for fluxes greater than 0.66 l/min, whereas $\delta\Delta T/\Delta T$ is a decreasing function of ΔT being $\delta\Delta T$ constant and equal to the thermocouple resolution [7] (0.1 °C). Combining eqs. (A.1) and (A.2) and noting that ΔT is proportional to the power supplied (Eqs. (1) and (2)), the dependence between the efficiency error and the power supplied has been obtained (see Fig. 29) assuming, on average, that 4% and 50% of the power supplied goes onto the cathode and anode,

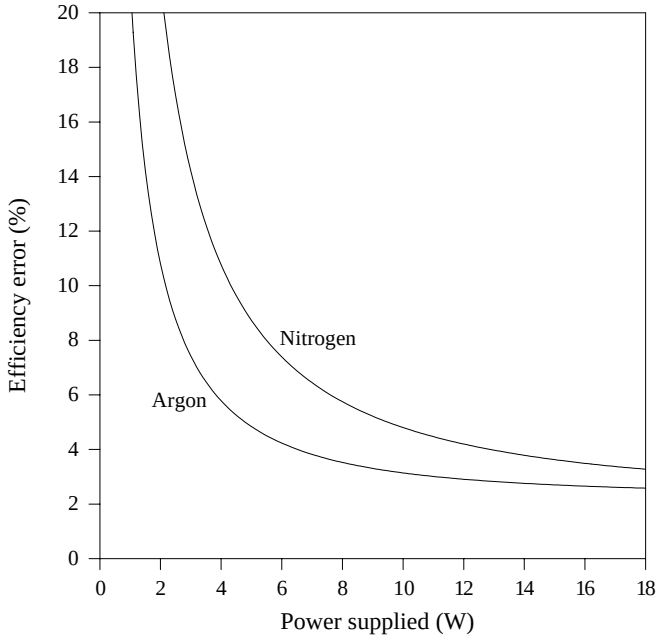

Fig. 29. Estimated efficiency error as a function of power supplied.

respectively, for argon and 2% and 30% for nitrogen. The efficiency error is less than 5% for power supplied greater than 4 kW in case of argon and 8 kW of nitrogen.

We wish to thank Fondazione Lombardia per l'Ambiente for the grants provided.

References

1. M. Nachman, Rev. Int. Htes Temp. Et Refract. **10**, 65 (1973).
2. A. Bokhari, M. Boulos, Can. J. Chem. Engin. **58**, 171 (1980).
3. R. Benocci, G. Braga, R. Florio, A. Galassi, S. Latorre, M. Paolicchio, M. Piselli, M. Sciascia, E. Sindoni, *ISPP Proceedings of "Thermal Plasmas for Hazardous Waste Treatment", Varenna (Italia) 4-6 September 1995* (World Scientific, 1996).
4. M. Boulos, P. Fauchais, E. Pfender, *Thermal Plasmas* (Plenum Press, New York, 1994).
5. G. Nutsch, *Proceedings of* 3rd *European Congress on "Thermal Plasma Processing", Aachen (Germany), September 19-21, 1994* (VDI Verlag).
6. R. Benocci, R. Florio, A. Galassi, M. Paolicchio, E. Sindoni, Nuovo Cimento D **19**, 911 (1997).
7. *LAIP: Design and calibration of an enthalpy probe*, work in progress.